Analysis of the Local Inelastic (Ballooning) Behaviour and Time-to-Failure of Zircaloy Claddings

V.K. Arya
University of Roorkee, Dept. of Mathematics, Roorkee 247 667, India

Abstract

A second order model, based on the perturbation theory, has been developed to analyse the ballooning behaviour of anisotropic Zircaloy claddings. The effects of anisotropy of Zircaloy,initial geometric imperfections in the cladding and temperature perturbations have been studied for various models. The time-to-failure calculated theoretically is found in good agreement with the corresponding experimental values from the FABIOLA burst tests. The anisotropic models explain the shortening of Zircaloy tubes observed in experiments. Anisotropy of Zircaloy is found to have a strengthening effect on the clad. The temperature perturbation affect the bulge growth more severely than the geometric imperfections.

Introduction

From a safety point of view, an understanding of the clad deformation is essential during a postulated loss of coolant accident (LOCA). Under LOCA conditions the cladding undergoes a temperature excursion and is subjected to lateral fission and filler gas pressure. Such conditions lead to the local bulging (ballooning) and rupture of the cladding. In order to ensure the safety of reactor and the supply of emergency coolant water to the core during LOCA, the cladding distortion should not cause the coolant flow blockage. Consequently an analysis of the local bulging (or ballooning) deformation of Zircaloy clads is of the utmost importance. The local bulging behaviour of the Zircaloy tubes has been the subject of several investigations /1-3/ in the recent past Kramer and Deitrich have enhanced a perturbation analysis to study the ballooning behaviour of clads. The Zircaloy is known to possess anisotropic properties /4,5,8/.

In the present paper a general second order anisotropic model, employing the Norton's law of creep, Prandtl - Reuss flow equations and based on anisotropic theory due to Hill/6/, has been developed. The effects due to geometric imperfections and temperature perturbations have been included and the conditions under which a geometric imperfection or thermal hot spot will grow unstably, investigated. From the analysis for the general second order anisotropic model, the analyses for i) second order isotropic model, ii) first order anisotropic model and iii) first order isotropic model have been deduced as particular cases. The numerical computations to predict the time-to-failure and ballooning behaviour of the clads, have been carried out and presented in the paper.

2. General Analysis

Modelling the cladding as a thin, slightly imperfect(initially perfect) cylindrical closed end shell without axial loading and following Arya /10/, the following equation of equilibrium may be obtained:

$$(LG - MF)\ \sigma_1^1 + (2M\sqrt{EG} - LF\sqrt{G/E} - NF\sqrt{E/G})\ \sigma_2^1 + (NE - MF)\ \sigma_2^2 = \frac{P}{h} H^2. \tag{1}$$

Here E,F,G are the first and L, M, N are the second fundamental magnitudes of the surface, $H^2 = EG - F^2$, h is the thickness of shell and P, the internal pressure. σ_1^1, σ_2^1 and σ_2^2 are the stresses.

The deformation is assumed to be composed of two components viz. an axisymmetric deformation and a local perturbation, denoted by e, and superimposed on the axisymmetric deformation. The stresses and other quantities are written as the sum of two components corresponding to unperturbed geometry (denoted by subscript c) and perturbed geometry (denoted by e) respectively. This latter component for the perturbed geometry tends to zero when there is no perturbation i.e. when e tends to zero.

Using expressions for E, F, G, L, M and N and the condition of incompressibility, one may obtain

$$\begin{aligned}
\sigma_{e\,1}^1 = {} & \frac{2P\lambda a^2}{h_a a_o}\frac{e}{a} + \frac{Pa^2\lambda}{h_o a_o}\frac{\partial^2 e/a}{\partial\theta_o^2} + \frac{a^2}{\lambda^2}\frac{\partial^2 e/a}{\partial z_o^2}\,\sigma_{zzc} + \frac{p\lambda a^2}{h_o a_o}\frac{e^2}{a^2} + \frac{P\lambda a^2}{h_o a_o}\frac{e}{a}\frac{\partial^2 e/a}{\partial\theta_o^2} \\
& + \left[\frac{Pa^2}{\lambda h_o a_o} + \frac{1}{\lambda^2}\sigma_{zzc}\right]\frac{e}{a}\,a^2\frac{\partial^2 e/a}{\partial z_o^2} + \frac{Pa^4}{\lambda h_o a_o}\left(\frac{\partial e/a}{\partial z_o}\right)^2 + \frac{P\lambda a^2}{h_o a_o}\left(\frac{\partial^2 e/a}{\partial\theta_o^2}\right)^2 \\
& + \left[\frac{Pa^2}{2\lambda h_o a_o} + \frac{1}{\lambda^2}\sigma_{zzc}\right]a^2\frac{\partial^2 e/a}{\partial\theta_o^2}\frac{\partial^2 e/a}{\partial z_o^2} + \frac{a^4}{2\lambda^4}\left(\frac{\partial^2 e/a}{\partial z_o^2}\right)^2\sigma_{zzc}
\end{aligned} \tag{2}$$

Here a is the radius of cylinder; r, θ, z are the cylindrical coordinates; subscript 'o' refers to initial values. λ is given by relation $z = \lambda z_o$ and $\sigma_{zzc} = 1/2\ \sigma_{c\,1} = 1/2\ Pa/h_c$. The true strain components are defined as

$$\begin{aligned}
\varepsilon_1^1 &= \varepsilon\theta_o = \ln\frac{a}{a_o} + \frac{a}{2a^2}\{2ae - e^2 + \left(\frac{\partial e}{\partial\theta_o}\right)^2\}, \\
\varepsilon_2^2 &= \varepsilon_{z_o} = \ln\lambda + \frac{1}{2\lambda^2}\left(\frac{\partial e}{\partial z_o}\right)^2, \\
\varepsilon_3^3 &= \varepsilon_r = \ln\frac{h_c}{h_o} + \frac{h_e}{h_c} - \frac{h_e^2}{h_c^2}\,;\ \varepsilon_2^1 = \varepsilon_{\theta_o z_o} = \frac{1}{\lambda a}\frac{\partial e}{\partial\theta_o}\frac{\partial e}{\partial z_o}\,.
\end{aligned} \tag{3}$$

Using the following set of constitutive equations

$$\frac{d\,\varepsilon_i^i}{dt} = \frac{1}{2\bar{\sigma}}\,S_i^i\,\frac{d\,\bar{\varepsilon}}{dt}\ ;\ i = 1, 2, 3 \text{(no summation)} \tag{4}$$

where $S_1^1 = \left[(A_2+A_3)\,\sigma_1^1 - A_3\,\sigma_2^2 - A_2\,\sigma_3^3\right]$ etc. and the effective stress

$$\bar{\sigma} = \frac{1}{\sqrt{2}}\left[A_1(\sigma_2^2 - \sigma_3^3)^2 + A_2(\sigma_3^3 - \sigma_1^1)^2 + A_3(\sigma_1^1 - \sigma_2^2)^2 + 2B_1(\sigma_2^1)^2\right]^{1/2} \tag{5}$$

together with Norton's law

$$\frac{d\bar{\varepsilon}}{dt} = K\,\bar{\sigma}^n \tag{6}$$

and the relation

$$\varepsilon_j^i = \varepsilon_{c\,j}^i + \varepsilon_{e\,j}^i \tag{7}$$

we obtain, for the unperturbed geometry, the following equations

$$\frac{d}{dt}\,\varepsilon_{c\,1}^{1} = \frac{1}{a}\,\frac{da}{dt} = \frac{K}{2}\,(2A_2 + A_3)\,\frac{Pa^2\lambda}{2h_o a_o}\,\tilde{\sigma}_c^{\,n-1} \tag{8}$$

$$\frac{d}{dt}\,\varepsilon_{c\,2}^{2} = \frac{1}{\lambda}\,\frac{d\lambda}{dt} = \frac{K}{2}\,(A_1 - A_3)\,\frac{Pa^2\lambda}{2h_o a_o}\,\tilde{\sigma}_c^{\,n-1}\,, \text{ etc.} \tag{9}$$

In these equations K and n are temperature dependent material constants and A_1, A_2, A_3 and B_1 are anisotropic constants. And for the perturbed geometry, we have

$$\frac{d}{dt}\,\varepsilon_{e\,1}^{1} = \frac{K}{2}\left[S_{11c}\,\sigma_{e\,1}^{1}\,\sigma_{e\,1}^{1} + S_{12c}\,\sigma_{e\,1}^{1}\,\sigma_{e\,2}^{2} + S_{22c}\,\sigma_{e\,2}^{2}\,\sigma_{e\,2}^{2} + S_{1c}\,\sigma_{e\,1}^{1} + S_{2c}\,\sigma_{e\,2}^{2}\right] + \frac{K_e}{2}\left[T_{oc} + S_{1c}\,\sigma_{e\,1}^{1} + S_{2c}\,\sigma_{e\,2}^{2}\right]\,; \text{ etc.} \tag{10}$$

The constant K_e in this equation enables the effects of temperature perturbations to be included in the analysis. After some analysis the differential equation governing the local bulging (ballooning) of the tube may be obtained. In Eq.(10) S_{11c}, S_{12c},.....etc. are the expressions involving the stresses for unperturbed geometry.

3. Solution

In order to analyse the effects of geometric and temperature perturbations and to investigate the conditions under which the geometric imperfections or temperature perturbations will lead to unstable growth of the clad, a solution of governing equation is required. To achieve this and guided by the form of the solutions for other instability problems like buckling, we assume that

$$\frac{e}{a} = B(t)\,\cos m\theta_o\,\cos\frac{\pi z_o}{L_o}\,;\ m \quad \text{integer} \tag{11}$$

Here L_o is the length of geometric imperfection. Using eq.(11) one obtains a non-linear ordinary differential equation of first order. This equation can be solved once the initial value of B i.e. $B(o) = B_o$ and the zeroth order solutions (i.e. the solutions for unperturbed geometry for a and λ, obtainable from eqs.(8) and (9), are known. Giving different sets of values θ_o, Z_o; the shape of the 'ballooned' part of the tube may be predicted. In the present paper the calculations only for the point $\theta_o = Z_o = 0$ which corresponds to the maximum growth of the bulge were carried out.

3.1 Second Order Isotropic Model

Substituting $A_1 = A_2 = A_3 = 1$, making necessary modifications and retaining terms upto order two in e, its derivatives and products, the equation governing the bulge growth in an isotropic tube may be obtained.

3.2 First Order Anisotropic Model

Neglecting the terms of order higher than one in e, the equation for the first order anisotropic model may be obtained.

3.3 First Order Isotropic Model

Substituting $A_1 = A_2 = A_3 = 1$ in the equations for the first order anisotropic model, the corresponding equations for first order isotropic model are obtained.

4. Numerical Calculations and Results

4.1 Geometric Imperfections

The values of n and ε, determined from FABIOLA burst tests are listed in Table II. The values of anisotropic constants at 525°C are taken from Hunt /8/ and are given in Table I. The values of other constants taken for numerical computations are: m = 1, a_o = 5.38 mm, h_o = 0.72 mm, B_o = 0.005 and the values of L_o are shown in graphs.

Table I

Material	A_1	A_2	A_3
ANISOTROPIC	0.748	0.384	1.868
ISOTROPIC	1.000	1.000	1.000

The time, t_f, for the failure of tube, defined as the time at which the radius a(t) (or parameter $\lambda(t)$) tend to infinity, may be obtained as:

$$t_f = 4\, h_o^n \,/\left[K\,(2A_2+A_3)\; n\;(2+K_1)\; K_2^{n-1}\;(Pa_o)^n\right] \tag{12}$$

Thus the time-to-failure depends on the anisotropy of the tube. The values for t_f have been listed in Table II.

4.2 Temperature Perturbations

The effect of temperature perturbations on bulge growth may be incorporated in the analysis through the constant K_e in the following manner. Using the Arrhenius type equation

$$K = K_o \exp\,(-\,Q/RT) \tag{13}$$

One may obtain, for small temperature variations about the mean temperature T_m, that

$$K_e = K\,(Q/R)\; T_e/T_m^2 \tag{14}$$

where Q/R ≃ activation temperature for self diffusion.

The calculations assuming a temperature perturbation of 10^oC, given by

$$T_e = 10\,\cos\theta_o\,\cos\,(\pi z_o/L_o) \tag{15}$$

have been carried out. The values of Q/R were taken from the data by Hoffmann /9/ and T_m = 750^oC. In the figures the following notations have been adopted:

$$\hat{a} = a(t)/a_o;\quad \lambda = \exp\,(z/z_o) \text{ and } \hat{e} = B(t)/B_o.$$

5. Discussion

The values of time-to-failure t_f, listed in Table II, for both anisotropic and isotropic models are found in good agreement with the experimental values, t_{fE}, for various FABIOLA burst tests. The time-to-failure for anisotropic clads is higher than that for an isotropic clad.

Figure 1 shows the plots of dimensionless radius (â) and axial displacements(λ) vs time t for the anisotropic and isotropic models. It is seen that while radial displacement increases continuously with time for both the cases; the axial displacement decreases with time for the anisotropic case and it remains constant for the isotropic case. Thus the shortening of Zircaloy clads, evidenced in experiments /7/ may be explained on the basis of the anisotropic model developed here. The effect of anisotropy on â is very small.

Figure 2 and 3 depict the values (logarithmic) of bulge for second and first order models for the anisotropic and isotropic cases respectively. It is seen that the values for second order models are greater than the corresponding values for the first order models. Initially this difference is small but it keeps on increasing with time and in the last few seconds it becomes very significant. Thus the initial geometric imperfection may result in higher values of bulge displacements and may also lead to the unstable growth of bulge.

The effect of anisotropy on second and first order models is shown in Figs.4 and 5. These figures show that the anisotropic claddings bulge at a much slower rate than the isotropic claddings. Figure 6 to 9 show the effects of temperature perturbations for anisotropic and isotropic claddings. It is seen from Figs. 6 and 7 that the values of the second order models are higher than the corresponding values for the first order models in both, anisotropic and isotropic, cases. The effect of temperature perturbation of even first order is seen to be much severe than that of a geometric imperfection. Thus the most probable source for the unstable growth of the cladding seems to be a thermal hot spot rather than a geometric imperfection.

Figures 8 and 9, exhibiting the effect of anisotropy on the bulge displacements owing to a temperature perturbation of 10^oC show that, both for second and first order models, these values for anisotropic models are much less than those for the isotropic models. The

anisotropy of clad therefore, seems to have a strengthening effect on clads.

6. Conclusions

On the basis of foregoing analysis and discussions, the following conclusions may be drawn:

1. The axial displacement (remaining constant for isotropic clads) is found to decrease with time for the anisotropic clads. Thus, the anisotropy of Zircaloy may be responsible for the shortening of Zircaloy clads, as evidenced experimentally/7/.

2. The values of bulge displacements for anisotropic models are always found to be less than the corresponding values for isotropic models. The anisotropy of clads, therefore, has a strengthening effect on them.

3. The values of bulge displacements due to temperature perturbations are seen to be much higher than the corresponding values due to an initial geometric imperfection. The most probable source of unstable growth of a cladding seems to be a thermal hot spot. The anisotropy is again found to have a strengthening effect on the clads.

7. References

/1/ LIN, E.I.H., "Analysis of the Ballooning Deformation of an Internally Pressurised Thin-Wall Tube During Fast Thermal Transient", Trans.4th International Conference on Structural Mechanics in Reactor Technology, California, Vol.C,Paper No.C 1/5,1977.

/2/ KRAMER, J.M. and DEITRICH,L.W.,"Cladding Failure by Local Plastic Instability", Argonne National Laboratory. Report No.ANL-77-95.

/3/ HAGRMAN, D.L.,"Zircaloy Cladding at Failure (BALON 2)EG & G Idaho. Report No.EGG-CDAP-5379.

/4/ LEE, D. et.al.,"Plasticity Theories and Structural Analysis of Anisotropic Metals - Zircaloys". EPRI. NP-500.

/5/ MAKI, H. and OOYAMA, M., "Plastic Deformation and Fracture Behaviour of Zircaloy - 2 Fuel Cladding Tubes under Biaxial Stress", J.Nuc.Sci. Technol.12,7,423-435,1975.

/6/ HILL, R., "The Mathematical Theory of Plasticity", Oxford (1950).

/7/ HOFMANN, P. und RAFF, S., "Verformungsverhalten von Zircaloy-4 Hullrohren unter Schutzgas im Temperturbereich zwischen 600 und 1200 °C", Report No.KfK 3168.

/8/ HUNT, C.E.L., "Anisotropic Theory and the Measurement and Use of the Anisotropic Factors for Zircaloy-4 Fuel Sheaths", Trans. 2nd International Conference on Structural Mechanics in Reactor Technology, London, Vol.1, Paper No.C 2/9.

/9/ HOFFMANN, M., Unpublished Data.

/10/ ARYA, V.K., "KfK Report", (1981).

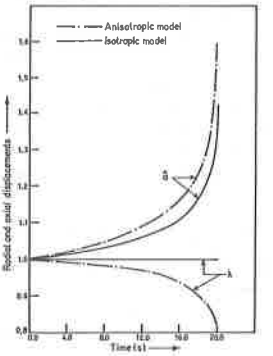

Fig.1 Dimensionless radial ($\hat{a}$) and axial (λ) displacements at different times t (Anisotropic and Isotropic models)

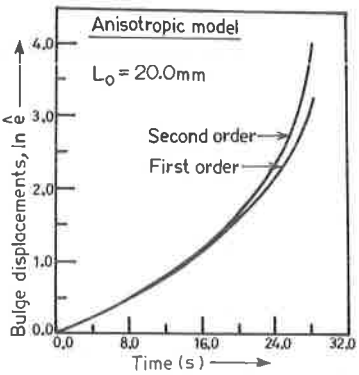

Fig.2

The values (logarithmic) of the bulge displacement $\ell n\ \hat{e}$, for the second and first order anisotropic models at different times t, with no temperature perturbation

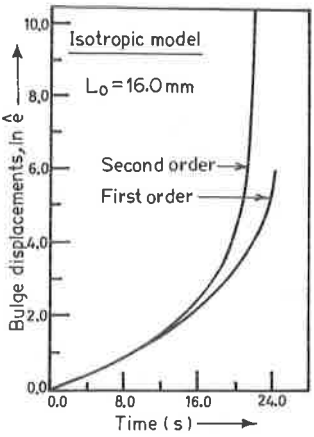

Fig.3

The values (logarithmic) of the bulge displacements, $\ell n\ \hat{e}$, for the second and first order isotropic models at different times t, with no temperature perturbation

No.	Test No.	n	$\dot{\epsilon}$	P (bar)	t_{f_E}(s)	ϵ_{f_E}(%)	Material	t_f(s)	t_{Rs}(s)	T_{BE}(°C)	Δ(%)
1.	17	6.550	0.00351	102.0	24.60	72 %	ANISO ISO	30.18 25.09	30.06 25.07	823.9	0.40 0.08
2.	19	6.785	0.00347	122.0	20.16	39.4 %	ANISO ISO	29.47 24.50	28.62 24.23	770.9	3.00 1.10
3.	25	5.432	0.00318	68.0	39.52	35 %	ANISO ISO	40.17 33.40	37.09 32.12	898.2	7.67 0.60
4.	26	5.380	0.001815	40.0	55.20	61 %	ANISO ISO	71.07 59.09	69.81 58.74	942.0	1.77 0.60
5.	28	4.675	0.00310	69.9	41.96	39.4 %	ANISO ISO	47.88 39.81	43.73 38.03	894.9	8.67 4.48
6.	29	5.700	0.00312	68.4	30.12	51.5 %	ANISO ISO	39.02 32.44	38.08 32.16	877.0	2.40 0.88
7.	31	6.600	0.003575	96.3	26.84	58.6 %	ANISO ISO	29.41 24.45	29.17 24.39	824.9	0.83 0.23
8.	33	5.400	0.003685	70.4	29.76	48.6 %	ANISO ISO	34.87 28.99	33.69 28.58	889.3	3.44 1.39
9.	34	6.760	0.00374	119.0	24.56	64.7 %	ANISO ISO	27.44 22.82	27.30 22.79	801.3	0.49 0.12

Explanation of Symbols : 1. n ⟶ exponent in creep law, 2. $\dot{\epsilon}$ ⟶ strain-rate (min), 3. P ⟶ pressure at the (minimum) strain-rate, 4. t_{f_E} ⟶ experimental value of time to failure, 5. ϵ_{f_E} ⟶ strain at failure, 6. ANISO ⟶ anisotropic; ISO ⟶ isotropic, 7. t_f ⟶ time to failure calculated from eq. (VI-1), 8. t_{Rs} ⟶ time when the strain (diametral) attains the value, ϵ_{f_E} 9. T_{BE} ⟶ experimental value of temperature at burst and 10. $\Delta = \frac{t_f - t_{Rs}}{t_f} \times 100$.

Table II Experimental data from FABIOLA burst tests; calculated time to failure for Anisotropic and Isotropic models etc.

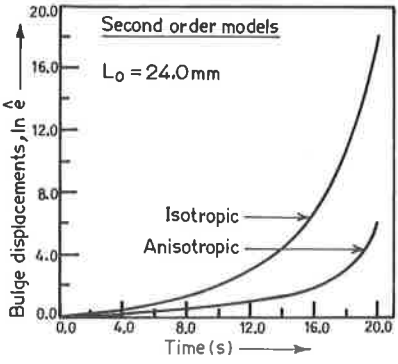

Fig.4 The values (logarithmic) of the bulge displacements ln $\hat{e}$, for second order isotropic and anisotropic models at different times t, with no temperature perturbation

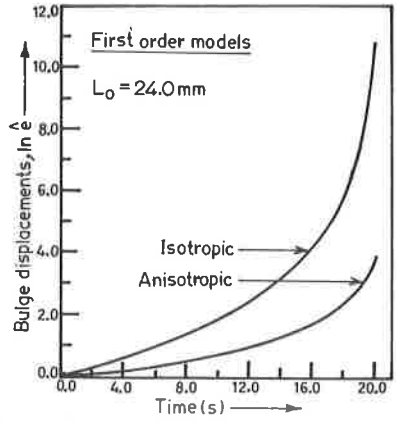

Fig.5 The values (logarithmic) of the bulge displacements ln $\hat{e}$, for first order anisotropic and isotropic models at different times t, with no temperature perturbation

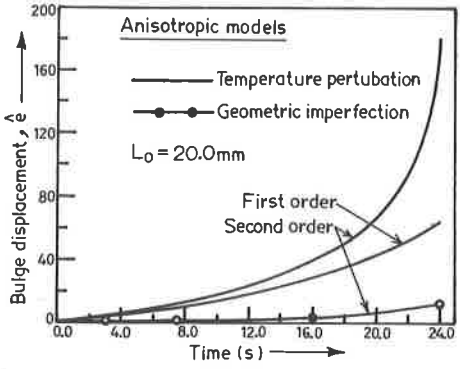

Fig.6 The values of bulge displacement $\hat{e}$, with temperature perturbation (10°C) at different times t (Anisotropic models)

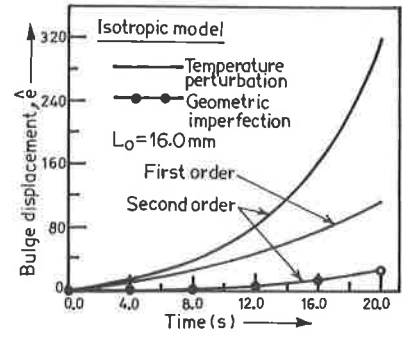

Fig.7 The values of bulge displacement $\hat{e}$, with temperature perturbation (10°C) at different times t (Isotropic models)

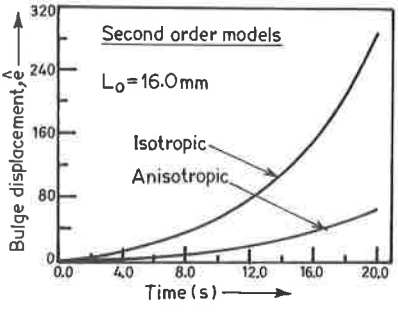

Fig.8 Effect of anisotropy on bulge displacement $\hat{e}$, with temperature perturbation (10°C), for second order models

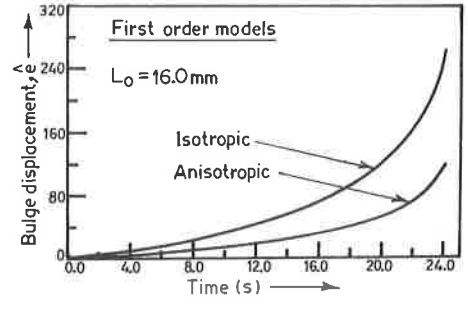

Fig.9 Effect of anisotropy on bulge displacement $\hat{e}$, with temperature perturbation (10°C), for first order models.